ASME Open Journal of Engineering
Online journal at:
https://asmedigitalcollection.asme.org/openengineering

A Procedure for the Static Design of Activated Carbon-Filled Air Springs

Stephan Breitenbach[1]
Machine Elements and Computer-Aided Product Development,
Department of Mechanical Engineering,
Helmut-Schmidt-University,
22043 Hamburg, Germany
e-mail: stephan.breitenbach@hsu-hh.de

Marcel Skoglund
Machine Elements and Computer-Aided Product Development,
Department of Mechanical Engineering,
Helmut-Schmidt-University,
22043 Hamburg, Germany
e-mail: marcel.skoglund@hsu-hh.de

Frank Mantwill
Professor
Machine Elements and Computer-Aided Product Development,
Department of Mechanical Engineering,
Helmut-Schmidt-University,
22043 Hamburg, Germany
e-mail: frank.mantwill@hsu-hh.de

Compared to conventional coil springs in passenger vehicles, air springs allow the vehicle body to be leveled independently of the load while maintaining an almost constant spring rate. However, while vehicle masses are increasing, the usable installation space for the suspension and especially the body springs is constantly decreasing as battery packs for electric vehicles tend to become larger. This leads to a conflict of objectives in the design of the air spring, as a low spring rate is mainly achieved by a large air volume in the spring. By introducing adsorbents into the enclosed air volume, the spring rate can be lowered while maintaining the same installation space. Conversely, it is possible to reduce the required installation space while achieving the specified stiffness. This work provides an analytical approach for the determination of the spring stiffness of air springs filled with activated carbon. In contrast to complex numerical approaches based on substitute tests, the presented method provides a simple and application-oriented stiffness prediction for adsorbent-filled air springs under quasi-static excitation. With the validation measurements presented, this provides a robust design tool for industrial use.
[DOI: 10.1115/1.4065527]

Keywords: design methods, modeling, suspensions, thermodynamics, vibration isolation, vibrations

1 Introduction

In the segments of mid-range and luxury vehicles, the rolling lobe air springs are an established alternative to conventional coil springs. An air suspension system enables load-independent adjustment of the ride height with constant spring characteristics. In the context of the growing popularity of electromobility, the requirements for vehicle suspensions are becoming increasingly complex. On the one hand, the vehicle masses are increasing due to the batteries. On the other hand, the available installation space for springs is becoming smaller. This leads to a conflict of objectives in the design of the air spring.

In this context, ways to lower the air spring stiffness under the same installation space are investigated [1]. By using adsorbents, air springs with the same physical installation space can be designed to be less stiff. In reverse, this makes it possible to reduce the installation space while maintaining the same target stiffness. This work shows a simple approach to predict the spring stiffness of activated carbon-filled air springs. The method presented focuses on an industrial application. It provides a simple analytical approach with measurements on the air spring itself without complex numerical simulations.

First, the function of the air spring and the principle of adsorption are explained. Based on the given context, an analytical model is derived. Subsequently, measurements for the model validation are presented and discussed.

2 Design and Function of the Air Spring

As shown in Fig. 1(*a*), the air spring consists of a fitting at the top, a rolling piston, and a sleeve. In order to maintain the internal pressure within the air spring, the sleeve is crimped to fitting and rolling piston. The sleeve forms a rolling fold due to the internal pressure. If an axial sleeve is used as in Fig. 1(*b*), an outer support is required to confine the sleeve [4]. The width of the rolling fold is therefore determined by the diameters and relative position of outer support and rolling piston.

In the air spring, air is the primary springy medium [5]. As with all springs, the spring stiffness is described as the ratio of the force F and the displacement s. In the air spring, the reaction force is a product of the effective area A_W and the gas pressure p [5]. The gas enclosed in the spring can be regarded as an ideal gas, as the temperature and pressure changes within the air spring are relatively small. According to Poisson's equation, the compression follows an isothermal change of state at slow deflections. The general equation for air spring stiffness according to Ref. [5] is shown in Eq. (1), where A_W describes the effective area, which equates the load-bearing and displacing areas. More information on the computation of the effective area may be found in Ref. [6].

$$c = np_0 \frac{A_W^2}{V_0} + (p_0 - p_u) \frac{\Delta A_W}{\Delta s} \tag{1}$$

Equation (1) shows that the filling pressure p_0 and the effective area A_W are directly proportional to the square of the spring rate c. The air spring volume V_0, on the other hand, is inversely proportional to

[1]Corresponding author.

Manuscript received January 18, 2024; final manuscript received May 8, 2024; published online May 30, 2024. Assoc. Editor: Joshua Summers.

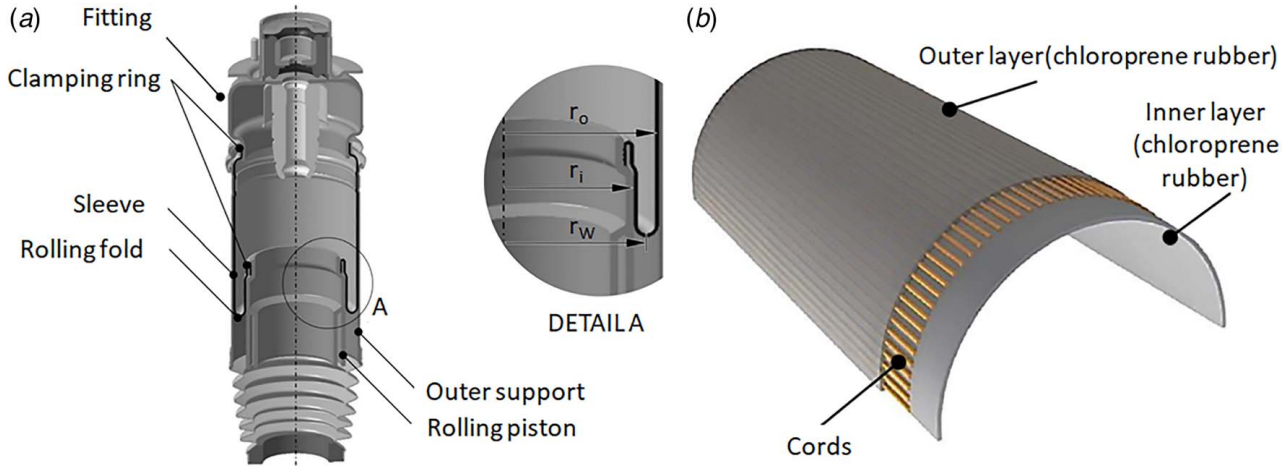

Fig. 1 Air spring: (*a*) simplified representation of the assembly (according to Ref. [2]) and (*b*) structure of an axial sleeve [3]

c [5]. The polytropic exponent n for air assumes a value between 1 for the isothermal change of state and 1.4 for the adiabatic change of state. With a constant effective area A_W, this results in an increase in stiffness by a factor of 1.4 during the transition from quasi-static to dynamic excitation, where the pressure p_0 is the absolute pressure prevailing in the air spring and p_u is the ambient pressure. If the air spring has a cylindrical rolling piston, as in Fig. 1(*a*), the second term of Eq. (1) can be neglected as it accounts for a change in effective area over deflection.

In order to meet the comfort requirements for air springs even in smaller installation spaces, innovative approaches are being investigated to make the spring smaller while maintaining the same properties. One way to reduce the spring stiffness without changing the geometric dimensions is to induce adsorbents into the air spring volume.

3 Basics of Adsorption

Adsorption is a case of sorption and occurs when gaseous substances or substances dissolved in liquids accumulate on a solid surface [7,8]. In the case of adsorption, a distinction is made between chemical and physical adsorption, as shown in Fig. 2.

Physisorption, as physical adsorption is called, binds the adsorbate (adsorbed substance) to the solid adsorbent by means of van der Waals forces [9,10]. In physisorption, it is possible for several layers to be adsorbed, a so-called multilayer adsorption or condensation [9]. In contrast to chemisorption, the process of physisorption is reversible [10]. The reverse process to adsorption is desorption, in which the adsorbed particles are released again at the surface.

The adsorption characteristics for a material are expressed in the form of isotherms [9]. They give the amount of adsorbed substance for the respective adsorption equilibrium with identical amounts of adsorbed and desorbed particles as a function of pressure for a given temperature. Adsorption releases energy in the form of heat and is therefore an exothermic process. The enthalpy of adsorption is made up of the enthalpy of condensation and enthalpy of binding [11]. Conversely, the energy is reabsorbed during desorption, so it is endothermic. Due to the low velocities during quasi-static excitation, the adsorption enthalpy can be neglected.

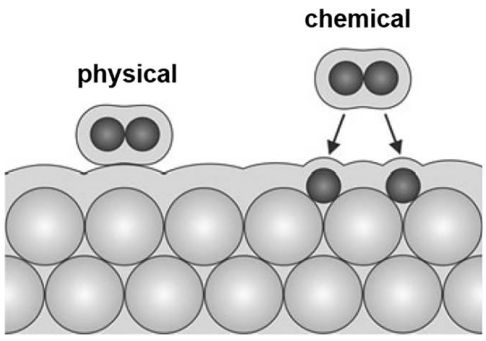

Fig. 2 Depiction of physisorption and chemisorption [9]

4 Derivation of an Analytical Model

Based on the principles of air springs and adsorption, this chapter derives an analytical model that enables a quasi-static design of air springs filled with activated carbon. On the one hand, this is intended to demonstrate a previously missing practical approach compared to the numerical method [1]. On the other hand, this reduces the time and number of preliminary tests for the spring design while maintaining sufficient accuracy.

For air springs with a cylindrical rolling piston, Eq. (1) is simplified by omitting the second term. Assuming that the simplified equation (1) for the air spring stiffness also applies to the adsorbed air volume, A_W and p_0 also have an effect on this volume. From this, a stiffness c_{AC} of the adsorbed air volume V_{ads} can be derived.

$$c_{AC} = np_0 \frac{A_W^2}{V_{ads}} \tag{2}$$

Due to the adsorbed air volume, the total volume of enclosed air in the spring increases and the stiffness decreases according to Eq. (1). Using the stiffnesses from Eq. (1) for the unfilled spring and Eq. (2) for the adsorption part results in a series connection of the stiffnesses. If the sleeve stiffness is also taken into account, which according to Ref. [12] must be considered as a parallel connection to the air volume, the equivalent diagram in Fig. 3 results.

c_{LF0} corresponds to the quasi-static air spring stiffness without activated carbon filling and c_{sleeve} corresponds to the stiffness caused by the sleeve. If c_{LF0} is not calculated but determined by measurements, the sleeve stiffness can also be neglected, as it is a constant addend to the total spring stiffness. This leads to Eq. (3), into which Eq. (2) can be inserted.

$$c_{total} = \frac{1}{(1/c_{LF0}) + (1/c_{AC})} \tag{3}$$

The ideal gas law applies to c_{AC} or V_{ads}:

$$p_0 V_{ads} = n_{ads} RT \tag{4}$$

The ideal gas law establishes the relationship between the adsorbed volume V_{ads} and the adsorbed amount of substance n_{ads}. The course of the adsorbed amount of substance over the pressure is described

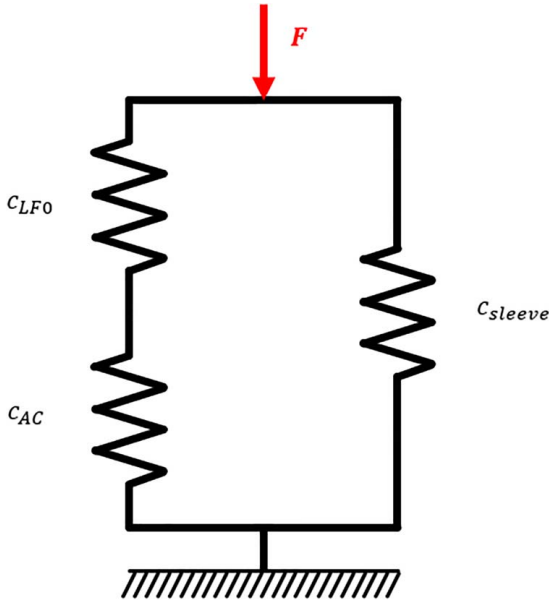

Fig. 3 Schematic diagram of the activated carbon-filled air spring in the quasi-static case

by the isotherm, which follows a type I isotherm curve for activated carbon in the pressure range investigated [1]. The Langmuir equation (5) applies to the curve [9,13,10].

$$n_{\text{ads}} = n_{\max} \frac{K_p p}{1 + K_p p} \tag{5}$$

K_p corresponds to the Langmuir coefficient and $n_{\max}$ to the maximum loading of the sorbent (assuming monolayer adsorption). By inserting Eq. (5) into Eq. (4) and rearranging to V_{ads}, you get Eq. (6). Since n_{ads} is given in mol/kg, the normalization can be made to the mass m_{AC} of the activated carbon monolith used.

$$V_{\text{ads}} = \frac{n_{\text{ads}} RT}{p_0} \cdot m_{\text{AC}} \tag{6}$$

If Eq. (6) is inserted into Eq. (2), Eq. (7) is obtained.

$$c_{\text{AC}} = \frac{A_W^2 p(1 + K_p p)}{n_{\max} K_p RT \cdot m_{\text{AC}}} \tag{7}$$

For the total stiffness according to Eq. (3), Eq. (8) applies:

$$c_{\text{total}} = \frac{1}{(1/c_{\text{LF0}}) + ((n_{\max} K_p RT m_{\text{AC}})/(A_W^2 p(1 + K_p p)))} \tag{8}$$

Equation (8) can now be used to determine the overall stiffness of activated carbon filled air springs. For this purpose, the static stiffness of the unfilled air springs, the isothermal coefficients of the activated carbon used, and their mass must be known.

5 Stiffness Investigations

For the stiffness characterization, measurements are carried out on a uniaxial hydropulse test rig as shown in Fig. 4. For air springs, Ref. [14] gives guidelines on how these measurements may be carried out. Since the influence of the adsorbent on the static spring stiffness is to be investigated, measurements are carried out at 0.001 Hz and an amplitude of ±40 mm.

The excitation of the spring results in a hysteresis loop in the force–displacement diagram due to the carbon-black-filled elastomer sleeve [4]. The stiffness of the spring c is calculated as the arithmetic mean of decompression and compression secant stiffnesses, according to Ref. [14].

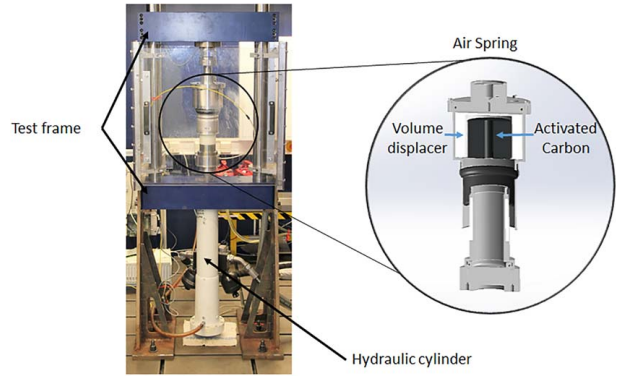

Fig. 4 Hydropulse test rig with development air spring (based on Ref. [3])

Table 1 Design of experiment—factors and stages at an amplitude of ± 40 mm and 0.001 Hz

Air spring volume (cm^3)	Pressure (bar)	Activated carbon mass (g)
1960	5	0
	7	121
2775	9	241
	11	367
3900	13	523
	–	669

The air spring used for characterization has an empty volume of 3900 cm^3 and an effective area of 92 cm^2. It is built with an axial sleeve and an outer support. The spring volume allows for adjustments between 1960 cm^3 and 2775 cm^3 using volume displacers as shown in Fig. 4.

5.1 Quasi-Static Stiffness Measurement. Activated carbon monoliths in pressed form are used as the object of investigation. All monoliths used have the same properties in terms of carbon type, binder type, and mixing ratios. The measurements are carried out with different masses, in different air spring volumes, at 5, 7, 9, 11, and 13 bar filling pressure. The pressure levels chosen represent the typical pressure range in the vehicle application.

In a first investigation, the stiffness is measured for an air spring volume of 2775 cm^3 at the pressures and activated carbon quantities listed in Table 1.

Using Eq. (3), the stiffness contribution from the activated carbon c_{AC} is calculated. The coefficients $n_{\max} = 0.690532$ mol/kg and $K_p = 0.0000021$/Pa in Eq. (7) are obtained from a non-linear regression with a least square error fit. The calculation was performed with MINITAB.[2] Comparing the measurement data to the results of Eq. (8) for the coefficients determined, a standard deviation of 2.4% with a maximum deviation of 7.5% is obtained.

After creating the model equation and determining the coefficients, the volumes 3900 cm^3 and 1960 cm^3 are measured at the same pressure levels and with the different amounts of activated carbon from Table 1. It should be noted that the spring volume of 1960 cm^3 can only be measured unfilled and with 121 g, 241 g, and 367 g activated carbon due to the reduced installation space caused by the volume displacer.

Applying the model from the first measurement with the volume of 2775 cm^3 to the measurements with the 3900 cm^3 and 1960 cm^3

[2]MINITAB is a software for the statistical analysis of data.

Table 2 Deviations between model and measurement depending on the different air spring volumes

	1960 cm^3	2775 cm^3	3900 cm^3
Average deviation (%)	0.7	1.3	2.2
Standard deviation (%)	1.0	2.4	2.2
Maximum deviation (%)	2.3	7.5	8.2

Table 3 Statistical coefficients for the Langmuir curve n_{max} and K_p

	1960 cm^3	2775 cm^3	3900 cm^3	Mean
n_{max} (mol/kg)	0.801526	0.690532	0.982257	0.763223
K_p (1/Pa)	1.21×10^{-06}	1.52×10^{-06}	6.34×10^{-07}	1.22×10^{-06}

volumes, the deviations in Table 2 between measurement and model result.

Table 2 shows that the model, which was determined using the 2775 cm^3 measurement, can be transferred to the other spring volumes. The maximum error for the tested configurations is always <10%.

The three measurement series are now examined individually. The computed coefficients per measurement series (air spring volume) are given in Table 3.

The isotherms derived from the coefficients in Table 3 are shown in Fig. 5. From Table 3 and Fig. 5, it can be seen that only results for the 3900 cm^3 measurement deviate significantly. Nevertheless, the deviation in the model approach remains below 10%. It should be noted at this point that the values of the coefficients determined from the statistics do not necessarily match the physical values. In order to investigate the influence of the compression ratio as cause for the deviations of the 3900 cm^3 measurements, an amplitude response analysis was carried out. This shows that the determined stiffnesses are parallel. Thus, the mean pressure p_0 can be used in the design according to Eq. (8).

6 Comparison of Isothermal Measurement

The isotherms determined from air spring measurements in Fig. 5 should be compared with the isotherms determined using volumetry. Established measurement methods for measuring isotherms are gravimetry and volumetry [15,16]. In the gravimetric measurement of adsorption isotherms, the change in weight caused by the adsorbed molecules is measured directly on the sample using a balance. Various gases and gas mixtures as well as temperature and pressure ranges can be set.

The volumetric sorption analysis is carried out using a gas pycnometer. The sorption analysis is carried out as a function of pressure, volume, and temperature in order to calculate the amount of gas that is removed from the gas phase [17]. The ideal gas law is used as a general basis for the calculation. A schematic diagram of the gas pycnometer used is shown in Fig. 6.

Adsorption isotherms of undried monoliths of masses 121 g, 239 g, and 367 g are derived in order to examine the activated carbon under near-use conditions. As it is not possible to measure undried samples using the available gravimeter (IsoSORP SA magnetic suspension balance), a measurement with a specifically built gas pycnometer is carried out. Knowing about a significant

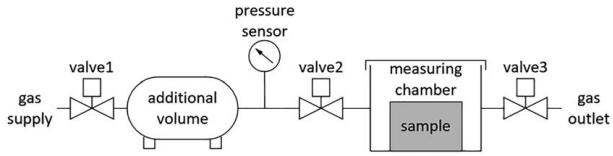

Fig. 6 Schematic diagram of the used gas pycnometer

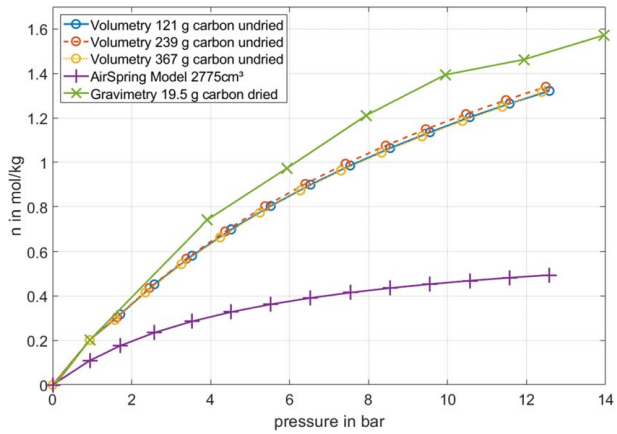

Fig. 7 Volumetric measurement taking into account the ambient pressure load

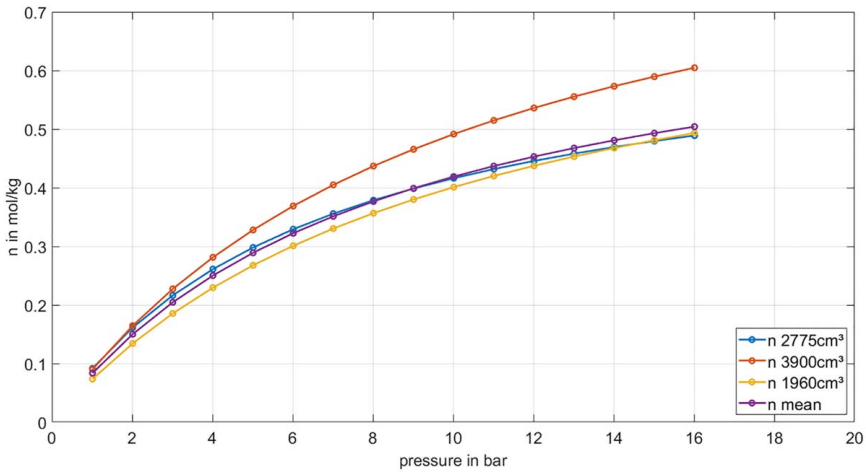

Fig. 5 Isotherms of the individual measurements compared to the determined mean value

Table 4 Isothermal coefficients from gas pycnometer and air spring measurements

	n_{gaspyc}	n_{LF}
n_{max} (mol/kg)	2.69787	0.690532
K_p (1/Pa)	7.68×10^{-07}	1.52×10^{-06}

Table 5 Model deviations of the reference air spring compared to the validation air spring

	Reference			Validation
Volume (cm^3)	1960	2775	3900	3090
Average deviation (%)	0.7	1.3	2.2	0.09
Standard deviation (%)	1.0	2.4	2.2	0.04
Maximum deviation (%)	2.3	7.5	8.2	1.10

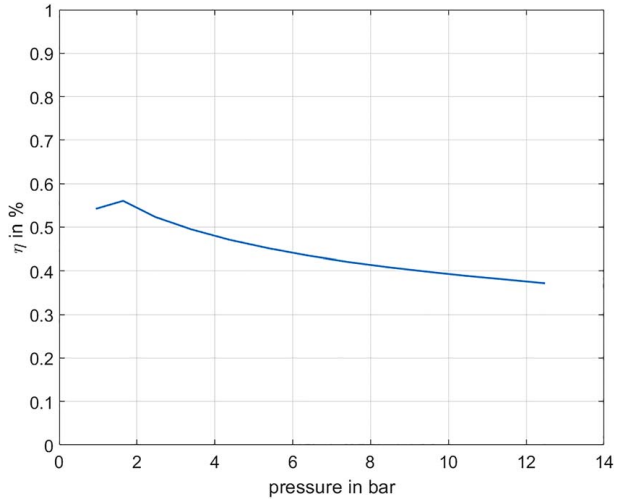

Fig. 8 Adsorption efficiency

influence of the moisture load at ambient pressure, gas pycnometer measurements are conducted relative to ambient pressure. In order to take the volumetric measurement into account in absolute terms, the substance adsorbed under ambient pressure is determined using gravimetry on dried samples. This value is then added to the isotherms as an offset. Using reference values from dried samples results in an overestimation of the isotherms, which is accepted here. The obtained results are given in Fig. 7, as well as the gravimetrically measured isotherm of the ground and dried sample. As the test chamber of the gravimeter is not large enough to hold the entire volume of a monolith, the sample mass is reduced to 19.5 g. The isotherms in Fig. 7 are shown in the net representation. It gives the additional amount of substance in the sample chamber. Further information on the different types of representation of isotherms can be found in Refs. [15,18].

Figure 7 shows a high degree of agreement between the adsorbed substance quantities for all masses investigated using volumetry. The gravimetrically determined isotherm is as well shown in Fig. 7. Here it can be seen that there is a slight deviation. This may be caused by the different sample quantities or by the moisture loading of the sample in the volumetry.

However, if the adsorption isotherms from the volumetry are compared to those from the air spring in Fig. 7, a clear deviation can be seen. As both the air spring measurement and the volumetry measurement were carried out under the same conditions, the cause cannot be attributed solely to the moisture loading of the activated carbon. This is confirmed by the small deviation between gravimetry and volumetry.

In the comparison between volumetry and air spring measurement, the coefficients in Table 4 result from the non-linear regression according to Eq. (5).

The data from Table 4 shows that the coefficients from the volumetric measurement and the air spring measurement differ significantly. From this it can be deduced, even if the coefficients from the air spring measurement were only determined statistically, that only a part of the activated carbon contributes to reducing the stiffness of the air spring.

The ratio of air spring measurement to volumetric measurement can be expressed as an efficiency value. The efficiency η as a function of pressure is shown in Fig. 8.

The course of the curve in Fig. 8 illustrates that in the pressure range between 6 and 12 bar (which is relevant for the air spring),

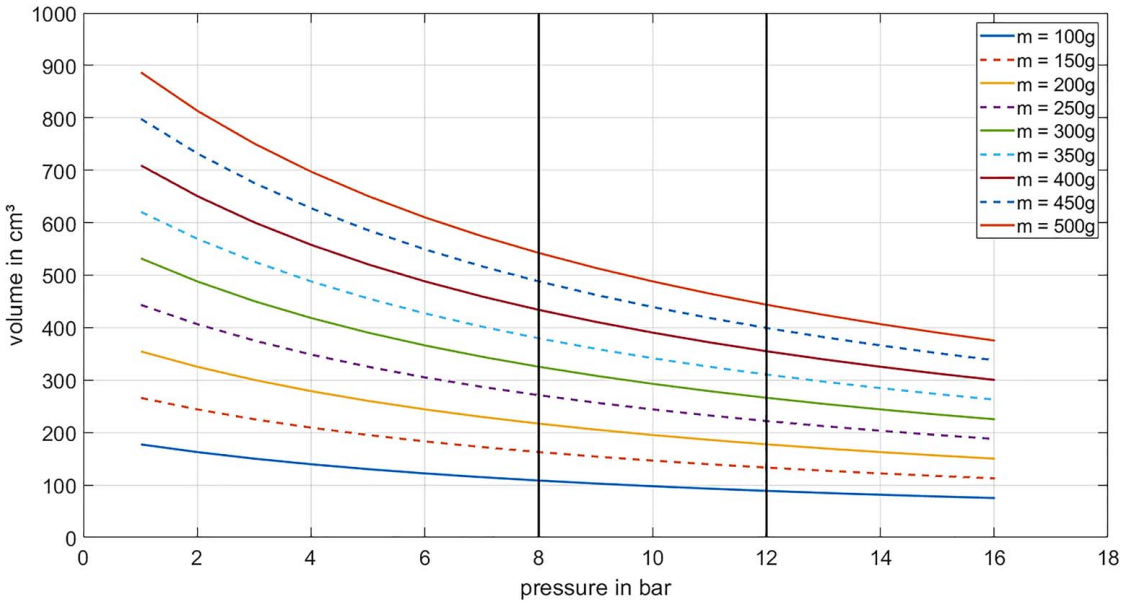

Fig. 9 Set of curves for volume savings

only around 45–38% of the adsorption capacity has an influence on the stiffness. The influence decreases with increasing pressure.

7 Applicability of the Model to Another Air Spring

In order to validate the derived model, it is applied to another spring. The spring used for validation has a physical air volume of 3090 cm^3 and an effective area of around 139 cm^2. The validation spring is filled with 367 g of activated carbon.

As with the reference air spring tests in the previous chapters, here too an empty measurement is preceded by the activated carbon test. The deviations between measurements and model for the validation air spring are given in Table 5. The model derived from the 2775 cm^3 studies is also used (Table 3).

Table 5 shows the model agreement for reference and validation measurements. This shows that the analytical approach developed provides a simple and good prediction without complex numerical simulations for the quasi-static stiffness design when results from a blank measurement are available.

8 Deriving a Volume Saving Chart

Especially in the early development phase, it is helpful to estimate the volume saving by activated carbon for an initial approximate design. The air volume adsorbed by the activated carbon is derived from the air spring measurements using the isotherm given in Fig. 7 and the ideal gas law (Eq. (4)) as a function of pressure and mass. Figure 9 provides absolute volume savings by means of adsorption for different activated carbon masses.

The typical operational pressure ranges for air springs lie between 8 and 12 bar. Assuming a maximum filling quantity of 500 g of the activated carbon configuration at hand, around 450 and 550 cm^3 of installation space volume can be saved while maintaining the same static spring characteristic.

9 Conclusion

In order to ensure the required stiffness and the associated comfort in the increasingly limited installation space of vehicle suspensions, new concepts are constantly being developed both in the area of conventional springs and air springs. In the area of air springs, the use of activated carbon is one way to make the spring less stiff while maintaining the same geometric volume.

This text describes a simple analytical method that makes it possible to predict the stiffness of air springs filled with activated carbon. To do this, it is necessary to know the basic stiffness of the air spring without activated carbon. This can be obtained through a blank measurement or based on a preliminary design. An isotherm is derived via a series of measurements in which the amount of activated carbon varied. This is done using a non-linear regression based on the derived equation. The determined isotherm is then used to derive the quasi-static spring stiffness. The method is validated with measurements on one activated carbon configuration.

Using the measurements and the analytical model, the additional air spring volume can be given as a function of activated carbon mass and filling pressure. This is particularly useful in the early phase of development. Reference measurements with other air spring volumes and an additional reference air spring module have shown that the model can be transferred.

Since vehicle springs are rarely subjected to solely static loads, the model presented here should be expanded to include the dynamic range of air springs.

Acknowledgment

The authors express their thanks to Vibracoustic SE & Co. KG, especially Mr. Koos, Mr. Zeeck, and the air spring Division for their cooperation as well as for their support of the research project in terms of content and funding.

Conflict of Interest

This article does not include research in which human participants were involved. Informed consent not applicable. This article does not include any research in which animal participants were involved.

Data Availability Statement

The datasets generated and supporting the findings of this article are obtainable from the corresponding author upon reasonable request.

References

[1] Breitenbach, S., Mantwill, F., and Sagert, A., 2023, "Dynamic System Behaviour of Adsorbent-Filled Air Springs," Int. J. Autom. Technol., **2021**(24), pp. 483–492.

[2] Hedrich, P., 2018, "Konzeptvalidierung einer aktiven Luftfederung im Kontext autonomer Fahrzeuge," Dissertation, Institut für Fluidsystemtechnik—FST, Technische Universität Darmstadt, Darmstadt.

[3] Breitenbach, S., Lips, M., and Mantwill, F., 2021, "Methoden zur Auslegung adsorbensgefüllter Luftfedern und zur Lebensdauervorhersage von Axialbälgen," Ilmenauer Federntag, Ilmenau.

[4] Lips, M., Breitenbach, S., Schmidt, P., and Mantwill, F., 2023, "Walkkräfte an Axialbälgen von Rollbalg-Luftfedern," Ilmenauer Federntag, Ilmenau.

[5] Vibracoustic, T., 2015, *Schwingungstechnik im Automobil*, Vogel Business Media GmbH & Co. K, Würzburg.

[6] Bedarff, T., 2016, "Grundlagen der Entwicklung und Untersuchung einer aktiven Luftfeder für Personenkraftwagen," Dissertation, Fachbereich Maschinenbau, Technische Universität Darmstadt, Darmstadt.

[7] Marsh, H., and Rodríguez-Reinoso, F., 2006, *Activated Carbon*, 1st ed., Elsevier, Amsterdam.

[8] Donau Carbon, 2018, "Aktivkohle-Und-Uhre-Anwendungen-2018," https://www.donau-carbon.com, Accessed May 21, 2024. https://www.donau-carbon.com/Downloads/aktivkohle.aspx.

[9] Job, G., and Rüffler, R., 2011, *Physikalische Chemie: Eine Einführung nach neuem Konzept mit zahlreichen Experimenten*, 1. aufl. ed., Vieweg+Teubner Verlag/Springer Fachmedien Wiesbaden GmbH Wiesbaden, Wiesbaden.

[10] Keller, J. U., and Staudt, R., 2005, *Gas Adsorption Equilibria: Experimental Methods and Adsorptive Isotherms*, 1st ed., Springer, Boston, MA.

[11] Schnabel, L., 2009, "Experimentelle Und Numerische Untersuchung der Adsorptionskinetik von Wasser an Adsorbens-Metallverbundstrukturen," Dissertation, Prozesswissenschaften,Technische Universität Berlin, Berlin.

[12] Löcken, F., 2017, "Für den Schwingungskomfort Relevante Eigenschaften von Rollbalg Luftfedern," Dissertation, Maschinenelemente und Rechnergestützte Produktentwicklung, Helmut-Schmidt-Universität, Hamburg.

[13] Kast, W., 1988, *Adsorption aus der Gasphase: Ingenieurwissenschaftliche Grundlagen und technische Verfahren*, VCH, Weinheim.

[14] Puff, M., and Pelz, P., 2009, "Entwicklung einer Prüfspezifikation zur Charakterisierung von Luftfedern," Vol. 223 of FAT-Schriftenreihe, VDA, Frankfurt am Main.

[15] Gumma, S., and Talu, O., 2010, "Net Adsorption: A Thermodynamic Framework for Supercritical Gas Adsorption and Storage in Porous Solids," Langmuir, **26**(22), pp. 17013–17023.

[16] Sing, K. S. W., Haul, R. A. W., Moscou, L., Pierotti, R. A., Rouquerol, J., and Siemienieniewska, T., 1985, "Reporting Physisorption Data for Gas/Solid Systems," Pure Appl. Chem., **57**(4), pp. 603–619.

[17] Talu, O., 1998, "Needs, Status, Techniques and Problems With Binary Gas Adsorption Experiments," Adv. Colloid Interface Sci., **76–77**(11), pp. 227–269.

[18] Brandani, S., Mangano, E., and Sarkisov, L., 2016, "Net, Excess and Absolute Adsorption and Adsorption of Helium," Adsorption, **2**(22), pp. 261–276.